Manganese oxidation induced by water table fluctuations in a sand column.

Claire E. Farnsworth,[1,2] Andreas Voegelin,[2] Janet G. Hering[2,3,4] *

[1]Division of Engineering and Applied Science, California Institute of Technology, Pasadena, CA 91125, [2]Eawag, Swiss Federal Institute of Aquatic Science & Technology, Dübendorf, Switzerland, CH-8600, [3]Institute for Biogeochemistry and Pollutant Dynamics, ETH, Zurich, Switzerland, [4]École Polytechnique Fédérale de Lausanne, School of Architecture Civil & Environmental Engineering, Lausanne, Switzerland

Corresponding author: Eawag, Überlandstrasse 133, CH-8600, Dübendorf, Switzerland

phone +41 (0)58 765 50 01, e-mail: janet.hering@eawag.ch

9 November 2011

TOC Art

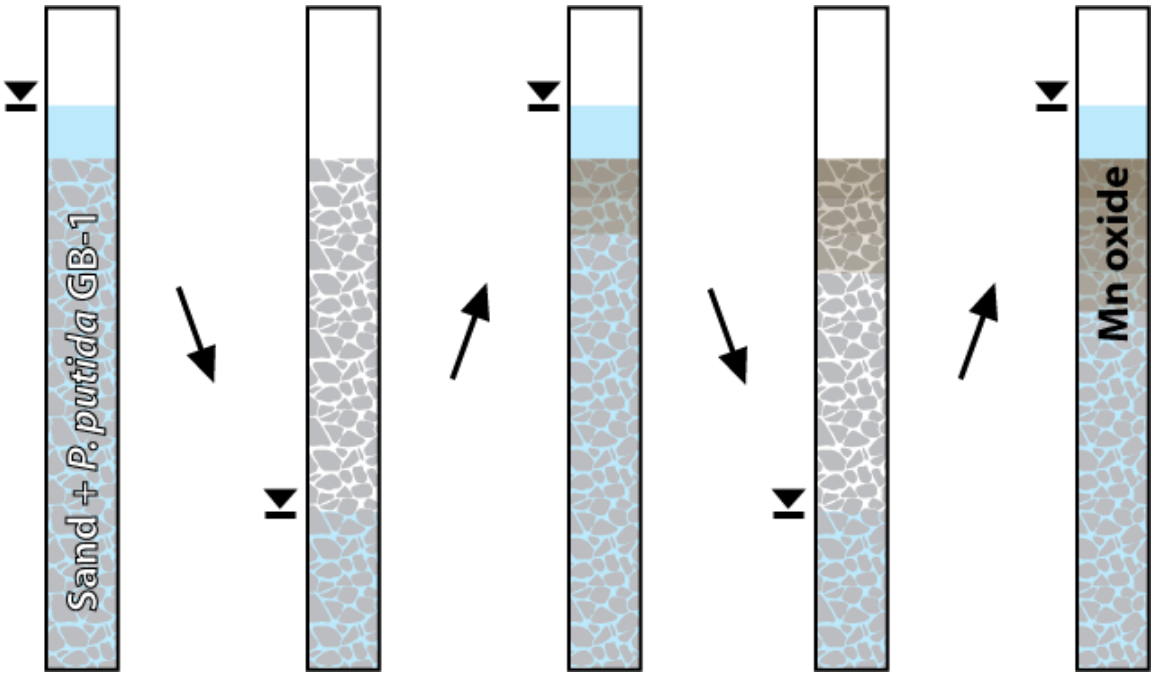

Abstract

On-off cycles of production wells, especially in bank filtration settings, cause oscillations in the local water table, which can deliver significant amounts of dissolved oxygen (DO) to the shallow groundwater. The potential for DO introduced in this manner to oxidize manganese(II) (Mn(II)), mediated by the obligate aerobe *Pseudomonas putida* GB-1, was tested in a column of quartz sand fed with anoxic influent solution and subject to 1.3 m water table changes every 30–50 h. After a period of filter ripening, 100 μM Mn was rapidly removed during periods of low water table and high dissolved oxygen concentrations. The accumulation of Mn in the column was confirmed by XRF analysis of the sand at the conclusion of the study, and both measured net oxidation rates and XAS analysis suggest microbial oxidation as the dominant process. The addition of Zn, which inhibited GB-1 Mn oxidation but not its growth, interrupted the Mn removal process, but Mn oxidation recovered within one water table fluctuation. Thus transient DO conditions could support microbially mediated Mn oxidation, and this process could be more relevant in shallow groundwater than previously thought.

Introduction

Groundwater extracted for drinking water often has manganese (Mn) and iron (Fe) concentrations above the WHO guidelines.[1-2] Post-extraction treatment in aerated sand filters is effective in decreasing Mn and Fe concentrations,[3] but it is possible that well operation could promote *in situ* Mn and Fe removal. On-off cycles of production wells in bank filtration sites, for example, cause oscillations in the local water table.[4] These fluctuations entrap air and deliver O_2 to the shallow groundwater.[5-7]

Subsurface Fe removal exploits this process in (partly) controlled systems: O_2-saturated groundwater is injected into the subsurface to oxidize Fe. Resumption of groundwater extraction from the well leads to Fe(II) sorption to Fe(III) oxides, and upon breakthrough of Fe, another pulse of O_2-saturated groundwater is injected. Succeeding cycles lead to an expansion of the zone of Fe removal and increased efficiency in the process, with no significant clogging.[8-10] It has been observed at some sites that subsurface Fe removal wells require less frequent rehabilitation than typical extraction-only groundwater wells.[11-12]

In comparison with Fe, the kinetics of Mn oxidation by O_2 are much slower and require microbial mediation at circumneutral pH.[13-14] The presence of dissolved Fe(II) also precludes significant Mn oxide accumulation, as Fe(II) rapidly reduces Mn oxides.[15] Mn removal in subsurface Fe removal sites is limited,[8, 11] and often Mn oxidation is omitted entirely from groundwater geochemical modeling.[16-17]

Nevertheless, the transient oxygen dynamics in well fields, especially bank filtration sites, suggest that the potential for *in situ* Mn oxidation exists, especially with low-Fe groundwater. This study tested whether water table fluctuations, similar in amplitude and frequency to those in a bank filtration site in Berlin, Germany,[4] could supply enough dissolved oxygen (DO) to oxidize Mn. *Pseudomonas putida* GB-1, an obligate aerobe and well-studied Mn oxidizing bacterium, was selected to colonize a column of quartz sand with anoxic influent, subject to >1 m water table fluctuations. The addition of 15 μM $ZnCl_2$ to the influent solution after 451 h tested the removal capacity of a trace cation in the presence of freshly formed Mn oxides and microbial biofilm.

Experimental Section

Reagents. All chemicals used were reagent grade and used without further purification. All water used was 18 MΩ-cm deionized water (Barnstead, Nanopure). Solutions were stored in plastic containers that had been acid-washed in 5% hydrochloric acid. All nitric acid solutions were made with trace metal grade HNO_3 (Merck Suprapur, 65%).

Bacterial Strain, Media, and Growth Conditions. *Pseudomonas putida* strain GB-1 (generously provided by C. M. Hansel, Harvard University) was grown in Luria Broth (LB) at room temperature (23.2°C) from LB agar plates. In early stationary phase, cells were harvested by centrifugation (20 minutes at 4,000g) and resuspended in MSTG growth medium[18] at pH 7.5: 2 mM $(NH_4)_2SO_4$, 0.25 mM $MgSO_4$, 0.4 mM $CaCl_2$, 0.15 mM KH_2PO_4, 0.25 mM Na_2HPO_4, 10 mM HEPES, 0.01 mM $FeCl_3$, 0.01 mM EDTA, 1 mM glucose, and 1 mL of trace metal solution (10 mg L^{-1} $CuSO_4 \times 5H_2O$, 44 mg l^{-1} $ZnSO_4 \times 7H_2O$, 20 mg l^{-1} $CoCl_2 \times 6H_2O$, and 13 mg l^{-1} $Na_2MoO_4 \times 2H_2O$). For Mn oxidation experiments, 0.1 mM $MnCl_2$ was added to MSTG media. For the column study, 5-l batches of MSTG were filter-sterilized (0.45 μm nitrocellulose, Whatman) and 1 mg l^{-1} NaBr was added to alternate batches, which had no effect on cell growth or Mn oxidation capacity. Growth of all bacteria was carried out with autoclaved or ethanol-rinsed materials under pure culture conditions.

Oxidation Assays. At the end of the column experiment, five batch experiments were used to compare the oxidizing activity of the column effluent, the column influent, and the GB-1 culture on agar plates at 4°C. 25 ml MSTG medium were added to sterile 50-ml centrifuge tubes.

Freshly prepared filter-sterilized medium was added to four tubes and degassed column influent solution was added to a fifth tube. Of the four tubes with fresh medium, the first was not inoculated, the second was inoculated from the GB-1 culture on a refrigerated plate, and the third and fourth were inoculated with 100 µl of the column effluent without and with 15 µM $ZnCl_2$ (summarized in Table S1). After 34 h shaken at 180 rpm at room temperature, samples were collected for OD_{600}. Samples were extracted first with 0.05 M $Cu(NO_3)_2$ in 0.05 M $Ca(NO_3)_2$, then with 0.5% hydroxylamine-HCl to give an approximate measure of Mn(II) and total Mn.[19] Extracted solutions were filtered (0.2 µm nitrocellulose, Whatman), diluted, and analyzed with ICP-MS (Agilent 7500cx).

Column Design and Flow Conditions. Plastic flanges were glued to the ends of an 8-cm inner diameter, 1.5-m length clear PVC pipe (wall thickness: 5 mm). Removable plastic plates were affixed to the flanges with screws, and sealed with a rubber O-ring between the plates and flanges. The influent and effluent ports were through the plastic plates at top and bottom. In addition, the column was fitted with three side ports (25, 50, and 75 cm from the column base) and a ventilation valve 7.5 cm from the column top. PVC tubing (wall thickness 2 mm) connected the influent port to a 10-l reservoir and the effluent port to a 3-way splitter open to the atmosphere. In downflow mode, water flowed by gravity into the column, and the height of the splitter controlled the height of the water table inside the column (Figure S1).

Ten kg uniformly sized quartz sand (Fontaineblau, BDH Prolabo, 0.24 mm average diameter) were slurry-packed in the column and held in place by a plastic mesh (pore size 0.088 mm) lining the bottom plate. The sand filled 122 cm of the column with a porosity of 0.39. The filled

column was then flushed in upflow mode with 3.5 l of 5% HCl, followed by >50 l of 1 mM NaBr solution bubbled with N_2 (99.999%, < 2 ppm O_2) to flush the acid and to remove the oxygen in the column; the side ports and ventilation valve were closed. Once the effluent dissolved oxygen (DO) was <10% of air saturation at room temperature, the column was switched from upflow to downflow, and the influent solution was switched to N_2-sparged MSTG without Mn. At this time, a 0.45-μm nitrocellulose filter membrane (Protran, Whatman) was added between the top plate and the O-ring. The sand was inoculated with 100 ml *P.putida* GB-1 culture (3.2×10^{11} cells l^{-1}) injected in the three ports and added directly through the top of the column. The system was allowed to equilibrate with no flow for 3 h, after which flow of N_2-sparged MSTG with Mn commenced (t = 0).

Flow through the column was maintained at an average of 3.2±1.2 l d^{-1}, or approximately one pore volume per day at the high water level. The visually observed water level inside the column was lowered from approximately 135 cm to 32 cm after 30-50 h by decreasing the splitter height, then raised again after 30-50 h by restoring the splitter height (Figure S1). The ventilation valve was open throughout the experiment to allow air entry in the drained and refilled pore volume. Water table fluctuations with flow continued for 615 h; short flow interruptions (<2 h) were required to degas fresh MSTG in the influent reservoir. Alternate batches of MSTG included 1 mg l^{-1} NaBr as a tracer to provide a qualitative assessment of the flow through the column over time. After 451 h (4 water table fluctuations), 15 μM $ZnCl_2$ was added to all subsequent influent solution.

The operation of the column was designed to minimize *P. putida* GB-1 taxis into the influent reservoir, as MSTG passed through a 0.45-μm filter and entered the column dropwise, mostly from the middle of the slightly sagging filter. Some MSTG, however, flowed intermittently along the column walls, and over 4 d, the bacteria were able to swim into the filter, most likely along these flow paths; Mn oxide and an opaque precipitate were observed along flow paths after 1 d of flow. Influent filters were therefore changed every 2-5 d when the clogged filters resulted in flow rates < 2.2 l d^{-1}. The absence of DO in the influent solution inhibited significant microbial growth (i.e., no visually observable turbidity), but the exposure of influent solution collected at the end of the experiment to air did yield cell growth (Table S1).

Sampling and Analyses. Samples were taken directly from the base of the column and from the collected effluent. Samples from the column base were analyzed for DO (polarographic DO probe, Thermo Electric) and pH (Ross Sure-Flow, Thermo Electric), and the volume of the collected effluent was volumetrically estimated to calculate the average flow rate. Filtered (0.2 μm cellulose acetate, VWR) and unfiltered subsamples of all effluent samples were diluted 100× with 1% HNO_3 for ICP-MS (Agilent 7500cx). The DO probe was calibrated before each sample; the pH electrode was calibrated daily.

At the end of the column experiment, the column was drained and frozen for 3 days to prevent further microbial growth. It was then thawed and the sand removed with a plastic core tube. Vertical sections of the sand (from the top of the column: 2×3.5 cm, 2.5 cm, and 9×12.5 cm in length) and one sample of unused sand were freeze-dried and milled for 90 s at 30 Hz with a ZrO_2 milling set (< 50 μm grain size, Retsch MM400), then pressed into 32-mm pellets for XRF

analysis (Spectro XEPOS). A subsample (180 mg) from the top section was thoroughly mixed with 20 mg of wax and pressed into a pellet (diameter: 1.3 cm) for analysis by Mn K-edge X-ray absorption near edge structure (XANES) and extended X-ray absorption fine structure (EXAFS) spectroscopy. Spectra were measured at the XAS beamline at the Angströmquelle Karlsruhe (ANKA, Karlsruhe, Germany). The Si(111) monochromator was calibrated by setting the first inflection point of the absorption edge of a Mn metal foil to 6539 eV. The sand pellet was measured at room temperature in fluorescence mode using a 5-element Ge solid state detector. Spectral data processing and linear combination fitting (LCF) were performed using the software code Athena.[20] The XANES spectrum was evaluated from 6530 to 6640 eV, the EXAFS spectrum from 2 to 10 $Å^{-1}$ (k-range relative to E_0 of 6550 eV). Reference spectra for LCF included aqueous Mn^{2+} (100 mM $Mn(NO_3)_2$; measured at SUL-X beamline at ANKA), δ-MnO_2 and hexagonal birnessite (phyllomanganate reference spectra from literature,[21] kindly provided by Sam Webb, SSRL).

Data Analysis. Hydraulic conductivity during the experiment was calculated with the Darcy equation:

$$K = v_D \frac{L}{\Delta H} \qquad (1)$$

where K is the hydraulic conductivity, v_D is the Darcy velocity equal to the volumetric flow rate divided by the cross-sectional area, L is the column length, and ΔH is the head difference between the column water level and the effluent splitter. The dispersion coefficient of the column was estimated from Br breakthrough with pulsed inlet concentration (Figure S2). Smooth breakthrough curves at constant water levels (i.e., 0-48 h, 190-234 h, 239-270 h, 326-358 h, and 560-592 h) were modeled in CXTFIT[22] to solve for the dispersion coefficient, D.

Pseudo-first-order Mn removal rates were estimated from the 1-D advective-dispersive transport equation:

$$\frac{\partial C}{\partial t} = D\frac{\partial^2 C}{\partial x^2} - \frac{v_D}{\varphi}\frac{\partial C}{\partial x} - kC \qquad (2)$$

where C is the dissolved Mn(II) concentration, D is the dispersion coefficient, φ is the porosity, and k is a pseudo-first-order removal rate. Solving for the local minimum in C(t) within each water table oscillation, with a Peclet number >>1 (advection dominates dispersion), this equation simplifies to:

$$\frac{\partial C}{\partial t} = -\frac{v_D}{\varphi}\frac{\partial C}{\partial x} - kC = 0 \qquad (3)$$

Integration over the column length yields the following expression for k:

$$k = -\frac{v_D}{\varphi \cdot L}\ln\frac{C}{C_0} \qquad (4)$$

where C/C_0 is the dimensionless concentration at the local minimum. Damköhler numbers, which assess the ratio of a reactive flux to advective flux, were calculated with this expression[23]:

$$Da = \frac{k \cdot C \cdot V}{Q \cdot C} \qquad (5)$$

where k is the pseudo-first-order rate coefficient [h^{-1}], V is the liquid volume in the column [l], and Q is the volumetric flow rate [$l\,h^{-1}$]; the Mn concentration, C, cancels out from the top and bottom of equation (5). For Da >3, a reaction can be assumed to reach completion.

Results and Discussion

Water Table Fluctuations and Dissolved Oxygen. Over a period of 615 h, the water table inside the column was oscillated 6 times from a high water level to a water level approximately

1.3 m lower and back to the high water level (Figure 1a); for clarity of description, one "fluctuation" or "oscillation" refers to a complete high-low-high water table cycle. The level of wetted sand was visually estimated to be ~32 cm above the column base, but the actual water table was calculated to be <5 cm based on the hydraulic conductivity of the column (calculated at the high water level). For sand with a 0.22-mm grain diameter and a porosity of 0.39, a 30-cm capillary fringe height is reasonable.[24] The hydraulic conductivity varied between 0.005 and 0.017 cm s^{-1} with no significant trend during column operation.

Air entered the unsaturated pore spaces when the water table was low, and was potentially entrapped when the water table was raised. The anoxic column influent acquired DO as the solution percolated downward through the unsaturated sand (maximum effluent DO of 3.6 mg l^{-1} = 42% saturation at 23.2°C), but did not acquire significant amounts of DO (< 1 mg l^{-1}) when the water table was high. Effluent DO levels are "net" DO concentrations, which reflect oxygen mass transfer from the gaseous phase to the dissolved phase as well as DO consumption by microbial respiration; the actual dissolved oxygen delivered to the aqueous phase is unknown. Some early problems with leaks through the side ports, as seen in the sharp drop in water level around 100 h, did not significantly affect DO dynamics.

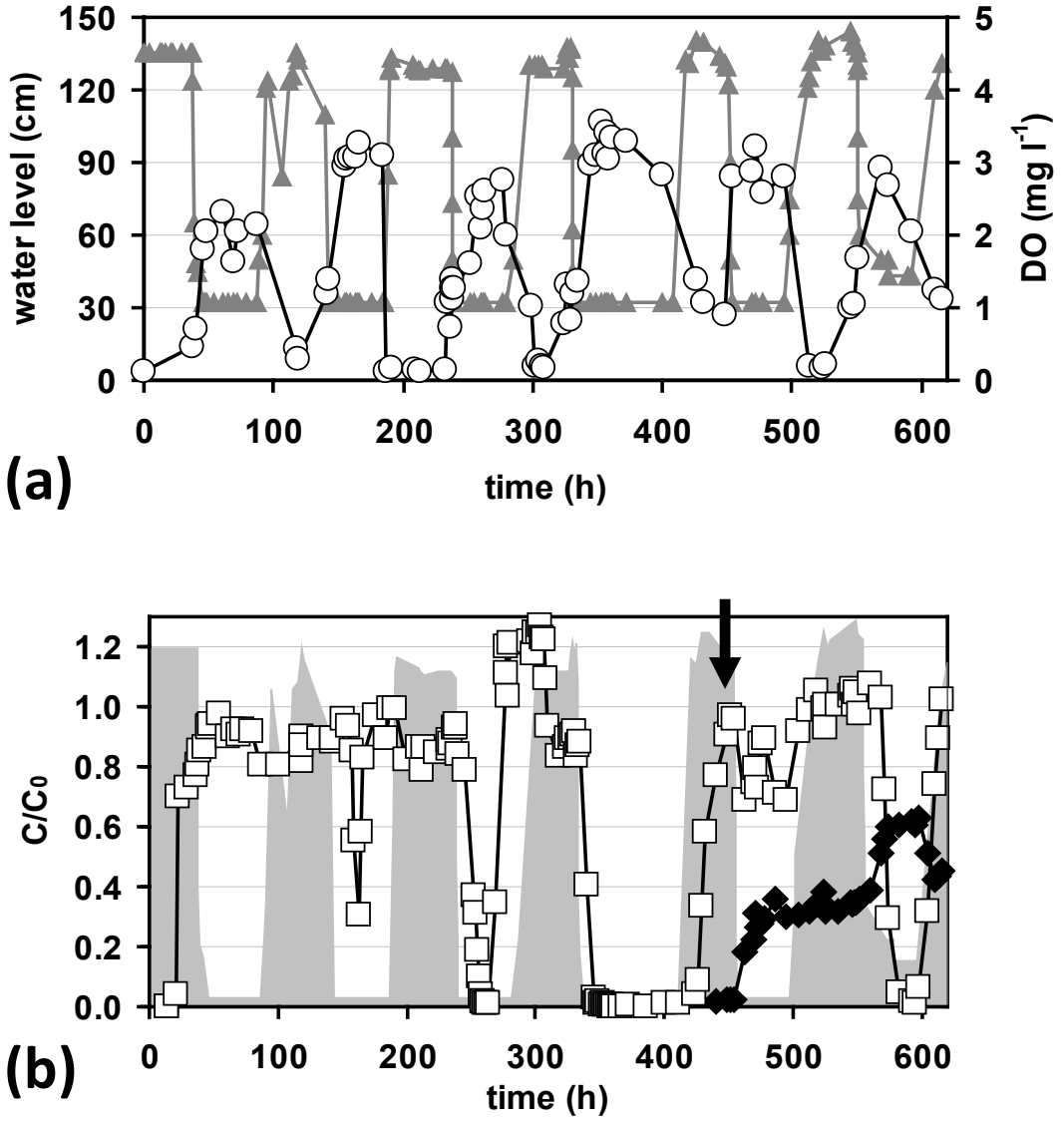

Figure 1. (a) Changes in the visible water level in the column (▲) and the effluent dissolved oxygen (○) over time. (b) Filtered relative effluent concentrations of Mn (□, C_0 = 100 μM) and Zn (◆, C_0 = 15 μM). The arrow denotes the addition of 15 μM Zn to the influent. For reference, the water level in the column is shown in the shaded profile (note the vertical scale is different than (a)).The residence time of the column was approximately 16.3 h.

Manganese Removal and Filter Ripening. After Mn uptake in the column in the first 1–2 pore volumes of influent (t < 30 h), Mn removal from the column influent coincides with lower water

levels, beginning 42 h after the first water table decrease (t=80 h, Figure 1b). The onset of Mn removal occurs 16, 8, and 4 h after the subsequent water level decreases (Table 1). The duration of the Mn removal also increases with 3 subsequent water level fluctuations, from approximately 14 h to 76 h in the fourth oscillation. Furthermore, the Mn removal increased to >99% by the third oscillation. Estimated pseudo-first order rate constants also increase with the first 4 oscillations (see further rate discussion below). These parameters all indicate a general improvement of the column's performance with time, or "filter ripening", which is commonly observed in water and wastewater treatment sand filters.[3, 25] Two regions of Mn washout ($C/C_0 > 1$) at 280 h and 513 h are likely a release of adsorbed Mn(II) in the column after a 10% decrease in influent Mn concentration. The formation of Fe oxide precipitates in those two batches of MSTG prior to the filter sterilization step was likely responsible for the inter-batch heterogeneity.

Table 1. Mn removal parameters for each water table oscillation.

oscillation	lag phase (h)	duration of removal (h)	minimum C/C_0	pore velocity (cm h^{-1})	k (h^{-1})	Da[a]
1	42	14	0.804	7.2	0.01	0.22
2	16	10	0.309	6.1	0.06	1.2
3	8	24	0.009	6.2	0.24	4.7
4	4	76	0.002	7.3	0.37	6.2
5[b]	28	17	0.688	7.5	0.02	0.41
6	19	29	0.011	6.5	0.24	4.5

[a] Damköhler number, the ratio of reactive flux to advective flux.

[b] 15 μM $ZnCl_2$ was added to the influent at the beginning of this oscillation.

As low water levels enhanced oxygen delivery to the aqueous phase, Mn removal at low water levels is consistent with Mn oxidation. Elevated DO was present in the effluent during the periods of greatest Mn removal. This is expected, since the column was colonized with *P. putida*

GB-1, an obligate aerobe whose ability to oxidize Mn is oxygen-dependent.[26] In batch studies, *P. putida* GB-1 commences Mn oxidation at the end of exponential phase, approximately 12 h after inoculation in MTSG at 30°C.[18] Orange-brown precipitates were visible on the sand at the top of the column after 44 h, and with subsequent water table fluctuations, they increased in spatial extent. XAS with linear combination fitting analysis further confirmed that the Mn in the topmost part of the column at the end of the experiment was Mn(IV) oxide (spectral combination of hexagonal birnessite and δ-MnO_2) with ca. 20% adsorbed Mn(II) (Figure S3, Table S2). XAS studies suggest *P. putida* MnB1, which is closely related to GB-1, and *Bacillus* sp. SG-1 both produce similar Mn oxides.[21, 27] Therefore, filter ripening processes for Mn removal in this experiment may be related to the development of an active zone of Mn oxidation, consistent with sand filters for Mn removal.[28]

Microbial biofilm growth and physiological adaptation to the column conditions likely contribute to the filter ripening, or enhanced Mn removal over time. Common in groundwater[29] and closely related to a strain isolated from Mn-oxide encrustations on water pipes (MnB1),[30] *P. putida* GB-1 can form biofilms attached to negatively charged surfaces (like silicates). Mn oxidation subsequent to attachment does not interfere with adhesion,[18] although it does result in a Mn oxide coating of the cell walls; complete coating of actively oxidizing microbial surfaces may account for the sharp increases in effluent Mn during filter ripening, especially in oscillations 2, 3, and 4. Based on the appearance of planktonic cells (and in some cases, biofilm and Mn oxides) in the column effluent, the initial inoculation of *P. putida* GB-1 quickly (<60 h) spread through the sand column. The absence of biofilm and Mn oxides observed in the collected effluent after three water table fluctuations suggests that the biofilm in the column became less susceptible to

1 washout over time. *P. putida* mt-2, a weak Mn oxidizer related to GB-1,[31] survived 24-h periods
2 of anoxia in batch experiments by up- and down-regulating gene expression based upon DO
3 availability,[32] further suggesting microbial adjustment to the column conditions was a critical
4 component of filter ripening.
5
6 The addition of 15 μM Zn at the beginning of the fifth water table oscillation (451 h) interfered
7 with the Mn removal process (only 31% removal). Although already present in MSTG at a low
8 concentration (150 nM), 15 μM Zn in the medium inhibited microbial Mn oxidation; cell growth
9 was slightly enhanced (Table S1). In previous batch experiments,[33] both Zn(II) and Ni(II)
10 inhibited Mn oxidation by *P. putida* GB-1 at concentrations higher than 20 μM. The authors
11 hypothesized that both Zn and Ni could compete with Mn(II) for binding sites at the oxidation
12 enzyme. In this study, the lag phase for removal increased from 4 h to 28 h, and the duration of
13 removal decreased from 76 h to 17 h (Table 1). Nevertheless, 99% Mn removal was restored
14 within one water table oscillation, with a lag phase of 19 h and a 29-h duration of removal. The
15 estimated pseudo-first-order rate constant similarly recovered to that of oscillation 3 (0.24 h^{-1}),
16 all despite the continued presence of Zn.
17
18 The Mn and Zn content in the column solids at the end of the experiment (Figure 2) lead to one
19 possible mechanism of microbial adjustment to the presence of Zn: the physical separation of Zn
20 removal and Mn removal zones. The Mn concentration had a steep gradient from 210 mg kg^{-1} at
21 the top of the column to 9 mg kg^{-1} in the 63-75 cm section, for an accumulation zone of
22 approximately 60 cm. Mn was above the 6 mg kg^{-1} sand background throughout the profile, and
23 the total Mn accumulation (XRF data, 2.42 mmol) was in excellent agreement with the total Mn

removal from solution ($C/C_0 \times Q$, 2.46 mmol). Zn also had a steep gradient from 8 mg kg^{-1} at the top of the column to <2 mg kg^{-1} in the 100-113 cm section, for an accumulation zone of approximately 22 cm. Below the accumulation zone, Zn was ≤1.5 mg kg^{-1}, the sand background. Zn accumulation (48 μmol) was in acceptable agreement with the total Zn removal from solution (93 μmol), considering that the Zn data approached the XRF practical quantitation limit (~1-2 mg kg^{-1}) and that the initial flush of acid through the column may have resulted in lower initial Zn in the column than measured in the unused (background) sand. A steep gradient in solid-phase P, perhaps indicative of biofilm, was also measured (Figure S4), whereas Br was constant with depth (not shown, 0.3 mg kg^{-1}). Thus, it is possible that Zn was adsorbed to older Mn oxides or biofilm material in the first cm of sand, then new Mn was oxidized below this zone.

Micro-scale zonation is also possible, as has been observed for Cu^{2+} in *P. putida* CZ1 biofilms.[34] In those biofilms, Cu^{2+} was confined to the surficial 40 μm of the biofilm, while Fe and Mn were distributed throughout the biofilm. Cu attachment to the biofilm matrix appeared to confer protection to the *P. putida* cells despite high mass loadings to the biofilm. Zn was similarly confined to the surficial 20 μm of *E. coli* PHL628 biofilms, although Fe and Mn distributions were not quantified.[35] The lack of Zn breakthrough (maximum $C/C_0 = 0.63$, Figure 1b) suggests the combined sorption capacity of the sand, Mn oxide, and biofilm was not reached. This is consistent with the lack of a maximum sorption affinity of the *P. putida* biomass for Zn in batch experiments.[36] The Zn release during the sixth oscillation (ca. 560-610 h) could be related to Zn complexes with organic compounds that are either soluble and produced under oxygenated conditions, or insoluble (in the biofilm matrix) and degraded under oxygenated conditions.

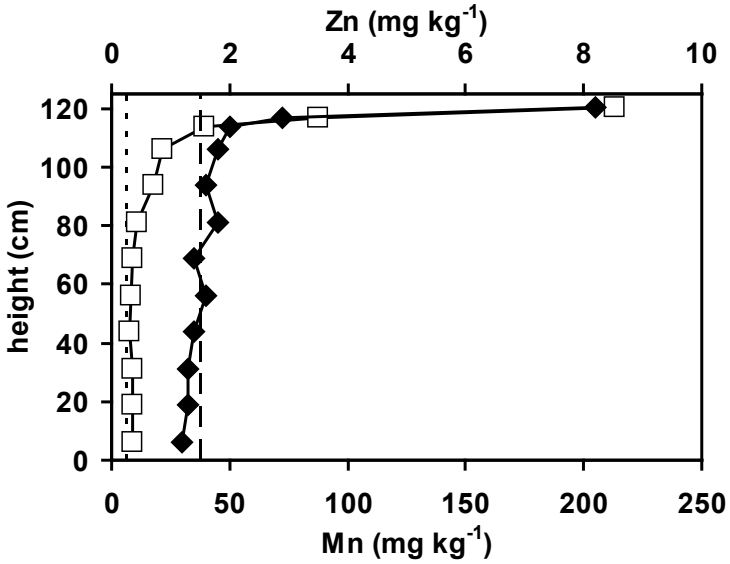

Figure 2. XRF profile of Mn (□) and Zn (◆) along the column at the end of the experiment. Dashed lines indicate the background Mn (short dashes) and Zn (long dashes) of unused sand. The plotted height is the average of the vertical section.

Rates of Mn Removal. Mn removal rates were estimated with 1-D advective-dispersive transport and a pseudo-first-order sink term. The dispersion coefficient in the column was between 1 and 7 $cm^2\ h^{-1}$, which corresponded to Peclet numbers between 120 and 700. For Pe >>1, the dispersion term in the transport equation could be omitted. For the minima in C vs. t $\left(\frac{\partial C}{\partial t} = 0\right)$, pseudo-first-order Mn removal rates then depended only on $C/C_{0,\,min}$, the length of the column, and the pore velocity (Table 1). These rates serve merely as a lower bound for the rate constant responsible for the decrease in C/C_0, since only for oscillation 4 was steady state clearly reached (Figure 1b). Furthermore, the minimum measurable value of C/C_0 was 0.001, based on the practical quantitation limit of the ICP-MS (0.9 nM) and 100-fold sample dilution. The Damköhler numbers for these rates ranged from 0.2 to 6.2, which suggests that for low rates

in oscillations 1, 2, and 5, the advective flux prevented the removal reaction from reaching completion. Otherwise, the rates in the column were not limited by flow conditions.

Manganese removal in the column is a net effect of multiple processes including abiotic reduction and oxidation by the microbial medium, microbial reduction and oxidation, and oxide-catalyzed oxidation. Photoreduction of Mn is assumed to be insignificant inside the sand column.[37 38]Mn-oxide-doped gels were used to assess the ability of the microbial medium and *P. putida* GB-1 to reduce Mn. Pseudo-first-order rate constants were 0.003 h^{-1} and 0.005 h^{-1} for the medium alone and the medium with cells, respectively (Table S3). These rate constants are in the range of O_2- and nitrate-reducing sediments (< 8 cm depth) in a German lake, measured with the same gel technique[39]. Oxidation by the microbial medium was insignificant (Figure S5).

Removal of Mn from solution by adsorption onto oxide surfaces is reported to occur with a half-life of 5 min,[38] which is insignificant on the multi-hour time scales of Mn removal; sorption to biofilm components is assumed to be similarly rapid. Below pH 9, abiotic oxidation rates are generally slow compared to microbial oxidation rates.[40] The effluent pH varied between 6.35 and 7.55, despite a constant influent pH of 7.5 (Figure S6), which further suggests that abiotic oxidation rates were irrelevant. Estimates of homogeneous[40] and surface-catalyzed (by both quartz sand[38] and Mn oxide[13]) Mn oxidation at pH 7 with full oxygen saturation indicate that abiotic oxidation is a minor contribution to the observed net oxidation rates (Table 2). Despite a large quantity of sand available to oxidize Mn, its low surface area (0.01 m^2 g^{-1} estimated for spherical grains) and low adsorption of Mn(II) at circumneutral pH result in a rate 3 orders of

magnitude lower than the lowest observed rate. Further details on the rate calculations are available in the supporting information.

Table 2. Potential rates of Mn oxidation and reduction in the column.

oxidation	homogeneous[40]	2×10^{-5} μM h^{-1}
	SiO_2-catalyzed[38]	2×10^{-3} μM h^{-1} [a]
	Mn oxide-catalyzed[13]	0.03 μM h^{-1} [b]
	P. putida GB-1[26]	240 μM h^{-1} [c]
	Leptothrix discophora SS1[41]	390 μM h^{-1} [c]
reduction	MSTG	0.3 μM h^{-1}
	MSTG + *P. putida* GB-1	0.5 μM h^{-1}
net observed oxidation rate	oscillation 1 (minimum)	1 μM h^{-1}
	oscillation 4 (maximum)	37 μM h^{-1}

[a] Rate assumes oxidation occurs throughout the column with 100% DO saturation.

[b] Rate uses the average final solid phase Mn (20 mg kg^{-1}) throughout the column with 100% DO saturation.

[c] Rate measured for ca. 10^{12} cells l^{-1} in Lept medium[41] with 100% DO saturation.

Thus the net observed oxidation rates (1-37 μM h^{-1}) are assumed to derive almost entirely from microbial oxidation. Although not directly confirmed at the end of the experiment, *P. putida* GB-1 is assumed to be the only microorganism in the column (Table S1). In shaken containers with dense (ca. 10^{12} cells l^{-1}) cultures, *P. putida* GB-1 has been shown[26] to oxidize Mn as fast as 240 μM h^{-1}. *Leptothrix discophora* SS1, another common Mn-oxidizing aerobe, oxidized Mn at rates up to 390 μM h^{-1} under the same batch conditions[41]. That these rates were measured in undefined Lept medium, which contains 0.5 g l^{-1} each of yeast extract and Casamino acids, accounts for some enhancement relative to the observed rates in defined minimal MSTG medium.

Comparison of the net observed oxidation rates with values in sand filters used for Mn removal is not straightforward. Although filter heights and residence times (τ) are generally reported, key

parameters such as porosity, specific surface area of the filter medium, biomass loading, and filter volume are frequently omitted. High variation in the residence times and initial Mn concentrations also make comparisons difficult. Reported rates range from 2.2 $\mu M\ h^{-1}$ (τ = 1.74 h; C_0 = 5 mg l^{-1}; sand with *L. discophora* SP-6)[28] to 1044 $\mu M\ h^{-1}$ (τ = 2-14 min; C_0 = 0.3–1.6 mg l^{-1}; polystyrene beads with Mn oxides and a mixed *Gallionella* and *Leptothrix* biofilm).[42] Manganese oxidation rates in mature filters could therefore exceed the net observed oxidation rates (τ = 16.3 h; C_0 = 5.5 mg l^{-1}).

Two additional factors that contribute to the slower measured rates are the pH and dissolved oxygen. General bacterial cell physiology may lead to the accumulation under anaerobic conditions of metabolites, which can then deliver protons upon reintroduction of oxygen.[43] The general inverse trend of pH and DO (Figures 1a and S6) suggests this may be the case. For *L. discophora* SS1, the maximum oxidation rate occurs at pH 7.5, with a steep decline to 30% of the maximum rate[44] or no oxidation at all[41] at pH 6.5. On the other hand, pH decreases were observed during both growth of *L. discophora* (due to CO_2 production) and Mn oxidation (the latter is predicted from stoichiometry as well)[41], so it is difficult to assess if the observed pH dynamics are merely a by-product of microbial growth and oxidation in the top cm of the column or if they actively limited a large portion of the microbial community.

Experiments with varying delivery rates of DO to GB-1 batch cultures revealed a strong dependence of Mn oxidation rate on the measured DO in late logarithmic phase.[26] Although its growth was unaffected by DO concentrations between 10-25% saturation (20°C), Mn oxidation required DO >14% in late logarithmic phase. The DO concentrations in that study reflect a

balance between the delivery rates (enhanced by variable shaking speed) and microbial consumption, not an absolute cutoff in oxygen concentration for Mn oxidation; even under rigorous shaking, the DO concentration in early- to mid-logarithmic phase was nearly zero.[26] Generally, in the presence of oxygen-consuming processes, oxygen mass transfer across the air-water interface is enhanced;[45] this is expected in the column as well. Interestingly, the maximum oxidation rate in early stationary phase corresponded with a DO of approximately 27% saturation (2.5 mg l^{-1}),[26] which is similar to the highest measured DO in the column effluent (3.6 mg l^{-1}). Literature studies of *P. putida* species that aerobically biodegrade organics similarly show decreasing degradation rates proportional to DO exhaustion, which rapidly recover upon reintroduction of oxygen.[32, 43, 46] Thus, the fluctuation of DO levels in the column between <1 mg l^{-1} and 3.6 mg l^{-1} (maximum) inhibited the microbial Mn oxidation rate, relative to those measured in fully oxygenated batches.

Implications for Groundwater Systems. The downflow setup, necessary to prevent *P. putida* taxis into the influent solution, limited the amount of air entrapment possible. This arrangement is more similar to rain percolation than to water table fluctuations in the field, for which rising water levels are expected to derive from lateral or upward water flux. Although the Peclet number and the frequency and amplitude of the water table fluctuations were chosen to be representative of bank filtration sites in Berlin, Germany,[4] the microbial medium and microbial community are not representative of field conditions. High amounts of phosphate (0.4 mM) and organic carbon (180 mg l^{-1} glucose) are unlikely in uncontaminated shallow aquifers; even in soils numerically dominated by *P. putida* species, they are generally <14% of culturable microbes.[29] The purpose of this study, however, was to test whether the DO supplied by water

table fluctuations is sufficient for Mn oxidation. Complete removal of 100 μM Mn(II) was indeed possible with the supplied DO; this Mn concentration is ten times higher than groundwater Mn concentrations considered to be problematic (or at least, which require post-extraction treatment) in Berlin[47] and Fredericton, Canada.[17] In general, Mn oxidation and transient DO concentrations are largely ignored in groundwater geochemical modeling,[16-17] but this study suggests that Mn oxidation in shallow groundwater could be more relevant than previously thought.

Key aspects that could affect the presence of a Mn oxidation zone in shallow groundwater include the source of the Mn(II), the depth of DO penetration, the depth of microbial Mn-oxidizing activity, and the amount of time for the microbial community to adjust to the available Mn. Vertical zonation of bank filtrate has been previously observed,[47] and if the Mn(II) is present below the depth of DO penetration and/or microbial Mn-oxidizing activity, very little *in situ* Mn oxidation potential exists. Microbial communities in sand filters for Mn removal require a notoriously long time (≥ 8 weeks) for startup,[3, 25] and Fe^{2+} and ammonium interfere with Mn-oxidation.[1, 25, 42] Even under ideal conditions, water treatment processes may still provide greater efficiency and faster rates than *in situ* Mn oxidation; removal rates in this study were 100× slower than those for aerated groundwater treatment columns with beads coated in Mn oxides and a mature, mixed *Gallionella* and *Leptothrix* biofilm community (1044 μM h^{-1}).[42] Furthermore, massive microbial growth and Mn oxide formation in the aquifer could lead to clogging, although no significant change in hydraulic conductivity was observed in this study. Nevertheless, engineering studies with longer time horizons and larger-amplitude and less

frequent water table oscillations, which would deliver more oxygen to the shallow groundwater, could perhaps optimize the *in situ* oxidation process to provide intransient Mn removal.

Acknowledgements

We acknowledge financial support from Eawag, an NSF Graduate Research Fellowship, and NSF EAR-3 0525387. Colleen Hansel and Deric Learman (Harvard University, Boston, USA) generously provided *P. putida* GB-1 and assisted in its cultivation. We acknowledge the Angströmquelle Karlsruhe (ANKA, Karlsruhe, Germany) for the provision of beamtime at the XAS and SUL-X beamlines and thank Stefan Mangold, Jörg Göttlicher and Ralph Steininger for their assistance during data collection. Sam Webb (Stanford Synchrotron Radiation Laboratory, Menlo Park, USA) is acknowledged for kindly providing reference XAS spectra for different Mn oxides.

Supporting Information Available

Schematic of experimental setup, results of oxidation assays, relative effluent Br concentrations, XAS results for sand in column, linear combination fitting of XAS spectra, XRF depth profile for P, pseudo-first order rate coefficients for Mn oxide reduction by *P. putida* GB-1, mass balance after the reduction assays, effluent pH values, and details of abiotic Mn oxidation rate calculations. This information is available free of charge via the Internet at http://pubs.acs.org/.

References

1. de Vet, W. W. J. M.; van Genuchten, C. C. A.; van Loosdrecht, M. C. M.; van Dijk, J. C., Water quality and treatment of river bank filtrate. *Drink. Water Eng. Sci.* **2010,** *3*, (1), 79-90.
2. Massmann, G.; Sültenfuß, J.; Dünnbier, U.; Knappe, A.; Taute, T.; Pekdeger, A., Investigation of groundwater residence times during bank filtration in Berlin: a multi-tracer approach. *Hydrol. Process.* **2007,** *22*, (6), 788-801.

3. Mouchet, P., From Conventional to Biological Removal of Iron and Manganese in France. *J. Am. Water Works As.* **1992,** *84*, (4), 158-167.
4. Massmann, G.; Sültenfuß, J., Identification of processes affecting excess air formation during natural bank filtration and managed aquifer recharge. *J. Hydrol.* **2008,** *359*, (3-4), 235-246.
5. Kohfahl, C.; Massmann, G.; Pekdeger, A., Sources of oxygen flux in groundwater during induced bank filtration at a site in Berlin, Germany. *Hydrogeol. J.* **2009,** *17*, (3), 571-578.
6. Beyerle, U.; Aeschbach-Hertig, W.; Hofer, M.; Imboden, D. M.; Baur, H.; Kipfer, R., Infiltration of river water to a shallow aquifer investigated with 3H/3He, noble gases and CFCs. *J. Hydrol.* **1999,** *220*, (3-4), 169-185.
7. Williams, M. D.; Oostrom, M., Oxygenation of anoxic water in a fluctuating water table system: an experimental and numerical study. *J. Hydrol.* **2000,** *230*, (1-2), 70-85.
8. Mettler, S.; Abdelmoula, M.; Hoehn, E.; Schoenenberger, R.; Weidler, P.; Gunten, U., Characterization of Iron and Manganese Precipitates from an In Situ Ground Water Treatment Plant. *Ground Water* **2001,** *39*, (6), 921-930.
9. Hallberg, R. O.; Martinell, R., Vyredox — In Situ Purification of Ground Water. *Ground Water* **1976,** *14*, (2), 88-93.
10. Appelo, C. A. J.; Drijver, B.; Hekkenberg, R.; de Jonge, M., Modeling *In Situ* Iron Removal from Ground Water. *Ground Water* **1999,** *37*, (6), 811-817.
11. van Halem, D.; de Vet, W.; Verberk, J.; Amy, G.; vanDijk, H., Characterization of accumulated precipitates during subsurface iron removal. *Appl. Geochem.* **2011,** *26*, (1), 116-124.
12. van Beek, C., Experiences with underground water treatment in the Netherlands. *Water Supply* **1985,** *3, Berlin "B"*, (2), 1-11.
13. Morgan, J. J., Manganese in natural waters and earth's crust: its availability to organisms. In *Manganese and its role in biological processes*, Sigel, A. S., Ed. Marcel Dekker, Inc.: New York, 2000.
14. Tebo, B. M.; Bargar, J. R.; Clement, B. G.; Dick, G. J.; Murray, K. J.; Parker, D.; Verity, R.; Webb, S. M., Biogenic Manganese Oxides: Properties and Mechanisms of Formation. *Annu. Rev. Earth Pl. Sc.* **2004,** *32*, (1), 287-328.
15. Postma, D.; Appelo, C. A. J., Reduction of Mn-oxides by ferrous iron in a flow system: Column experiment and reactive transport modeling. *Geochim. Cosmochim. Ac.* **2000,** *64*, (7), 1237-1247.
16. Kübeck, C.; Hansen, C.; Bergmann, A.; Kamphausen, S.; König, C.; van Berk, W., Model Based Raw Water Quality Management – Manganese Mobilization Induced by Bank Filtration. *Clean* **2009,** *37*, (12), 945-954.
17. Thomas, N. E.; Kan, K. T.; Bray, D. I.; MacQuarrie, K. T. B., Temporal Changes in Manganese Concentrations in Water from the Fredericton Aquifer, New Brunswick. *Ground Water* **1994,** *32*, (4), 650-656.
18. Parikh, S. J.; Chorover, J., FTIR Spectroscopic Study of Biogenic Mn-Oxide Formation by *Pseudomonas putida* GB-1. *Geomicrobiol. J.* **2005,** *22*, (5), 207 - 218.
19. Warden, B. T.; Reisenauer, H. M., Fractionation of Soil Manganese Forms Important to Plant Availability. *Soil Sci. Soc. Am. J.* **1991,** *55*, (2), 345-349.
20. Ravel, B.; Newville, M., ATHENA, ARTEMIS, HEPHAESTUS: data analysis for X-ray absorption spectroscopy using IFEFFIT. *J. Synchrotron Rad.* **2005,** *12*, (4), 537-541.

21. Webb, S. M.; Tebo, B. M.; Bargar, J. R., Structural characterization of biogenic Mn oxides produced in seawater by the marine *Bacillus* sp. strain SG-1. *Am. Mineral.* **2005,** *90*, (8-9), 1342-1357.
22. Toride, N.; Leij, F. J.; van Genuchten, M. *The CXTFIT code for estimating transport parameters from laboratory or field tracer experiments - Version 2.0*; U.S. Salinity Laboratory Report No. 137; Riverside, CA, 1995.
23. Battersby, S.; Teixeira, P. W.; Beltramini, J.; Duke, M. C.; Rudolph, V.; Diniz da Costa, J. C., An analysis of the Peclet and Damkohler numbers for dehydrogenation reactions using molecular sieve silica (MSS) membrane reactors. *Catalysis Today* **2006,** *116*, (1), 12-17.
24. Lohman, S. W. *Ground-Water Hydraulics*; Professional Paper 708; U.S. Geological Survey: Washington D.C., 1972.
25. Frischherz, H.; Zibuschka, F.; Jung, H.; Zerobin, W., Biological elimination of iron and manganese. *Water Supply* **1985,** *3, Berlin 'B'*, (1), 125-136.
26. Okazaki, M.; Sugita, T.; Shimizu, M.; Ohode, Y.; Iwamoto, K.; de Vrind-de Jong, E. W.; de Vrind, J. P.; Corstjens, P. L., Partial purification and characterization of manganese-oxidizing factors of *Pseudomonas fluorescens* GB-1. *Appl. Environ. Microbiol.* **1997,** *63*, (12), 4793-4799.
27. Villalobos, M.; Toner, B.; Bargar, J.; Sposito, G., Characterization of the manganese oxide produced by *Pseudomonas putida* strain MnB1. *Geochim. Cosmochim. Ac.* **2003,** *67*, (14), 2649-2662.
28. Vandenabeele, J.; de Beer, D.; Germonpré, R.; Verstraete, W., Manganese oxidation by microbial consortia from sand filters. *Microbial Ecol.* **1992,** *24*, (1), 91-108.
29. DePalma, S. R. Ph.D. Thesis. Manganese Oxidation by *Pseudomonas putida*. Harvard University, 1993.
30. Caspi, R.; Tebo, B. M.; Haygood, M. G., c-Type Cytochromes and Manganese Oxidation in *Pseudomonas putida* MnB1. *Appl. Environ. Microbiol.* **1998,** *64*, (10), 3549-3555.
31. Francis, C. A.; Tebo, B. M., *cumA* Multicopper Oxidase Genes from Diverse Mn(II)-Oxidizing and Non-Mn(II)-Oxidizing *Pseudomonas* Strains. *Appl. Environ. Microbiol.* **2001,** *67*, (9), 4272-4278.
32. Martinez-Lavanchy, P. M.; Muller, C.; Nijenhuis, I.; Kappelmeyer, U.; Buffing, M.; McPherson, K.; Heipieper, H. J., High Stability and Fast Recovery of Expression of the TOL Plasmid-Carried Toluene Catabolism Genes of *Pseudomonas putida* mt-2 under Conditions of Oxygen Limitation and Oscillation. *Appl. Environ. Microbiol.* **2010,** *76*, (20), 6715-6723.
33. Brouwers, G.-J.; de Vrind, J. P. M.; Corstjens, P. L. A. M.; Cornelis, P.; Baysse, C.; de Vrind-de Jong, E. W., *cumA*, a Gene Encoding a Multicopper Oxidase, Is Involved in Mn^{2+} Oxidation in *Pseudomonas putida* GB-1. *Appl. Environ. Microbiol.* **1999,** *65*, (4), 1762-1768.
34. Chen, G.; Chen, X.; Yang, Y.; Hay, A. G.; Yu, X.; Chen, Y., Sorption and Distribution of Copper in Unsaturated *Pseudomonas putida* CZ1 Biofilms as Determined by X-Ray Fluorescence Microscopy. *Appl. Environ. Microbiol.* **2011,** *77*, (14), 4719-4727.
35. Hu, Z.; Hidalgo, G.; Houston, P. L.; Hay, A. G.; Shuler, M. L.; Abruna, H. D.; Ghiorse, W. C.; Lion, L. W., Determination of Spatial Distributions of Zinc and Active Biomass in Microbial Biofilms by Two-Photon Laser Scanning Microscopy. *Appl. Environ. Microbiol.* **2005,** *71*, (7), 4014-4021.

36. Toner, B.; Manceau, A.; Marcus, M. A.; Millet, D. B.; Sposito, G., Zinc Sorption by a Bacterial Biofilm. *Environ. Sci. Technol.* **2005,** *39*, (21), 8288-8294.
37. Xyla, A. G.; Sulzberger, B.; Luther, G. W.; Hering, J. G.; Van Cappellen, P.; Stumm, W., Reductive dissolution of manganese(III, IV) (hydr)oxides by oxalate: the effect of pH and light. *Langmuir* **1992,** *8*, (1), 95-103.
38. Davies, S. H. R.; Morgan, J. J., Manganese(II) oxidation kinetics on metal oxide surfaces. *J. Colloid Interf. Sci.* **1989,** *129*, (1), 63-77.
39. Farnsworth, C. E.; Griffis, S. D.; Wildman, J. R. A.; Hering, J. G., Hydrous Manganese Oxide Doped Gel Probe Sampler for Measuring In Situ Reductive Dissolution Rates. 2. Field Deployment. *Environ. Sci. Technol.* **2009,** *44*, (1), 41-46.
40. Morgan, J. J., Kinetics of reaction between O_2 and Mn(II) species in aqueous solutions. *Geochim. Cosmochim. Ac.* **2005,** *69*, (1), 35-48.
41. Boogerd, F. C.; de Vrind, J. P., Manganese oxidation by *Leptothrix discophora*. *J. Bacteriol.* **1987,** *169*, (2), 489-494.
42. Katsoyiannis, I. A.; Zouboulis, A. I., Biological treatment of Mn(II) and Fe(II) containing groundwater: kinetic considerations and product characterization. *Water Res.* **2004,** *38*, (7), 1922-1932.
43. Balcke, G. U.; Turunen, L. P.; Geyer, R.; Wenderoth, D. F.; Schlosser, D., Chlorobenzene biodegradation under consecutive aerobic–anaerobic conditions. *FEMS Microbiol. Ecol.* **2004,** *49*, (1), 109-120.
44. Zhang, J.; Lion, L. W.; Nelson, Y. M.; Shuler, M. L.; Ghiorse, W. C., Kinetics of Mn(II) oxidation by *Leptothrix discophora* SS1. *Geochim. Cosmochim. Ac.* **2002,** *66*, (5), 773-781.
45. Haberer, C. M.; Rolle, M.; Liu, S.; Cirpka, O. A.; Grathwohl, P., A high-resolution non-invasive approach to quantify oxygen transport across the capillary fringe and within the underlying groundwater. *J. Contam. Hydrol.* **2011,** *122*, (1-4), 26-39.
46. Bauer, R. D.; Rolle, M.; Kürzinger, P.; Grathwohl, P.; Meckenstock, R. U.; Griebler, C., Two-dimensional flow-through microcosms - Versatile test systems to study biodegradation processes in porous aquifers. *J. Hydrol.* **2009,** *369*, (3-4), 284-295.
47. Massmann, G.; Nogeitzig, A.; Taute, T.; Pekdeger, A., Seasonal and spatial distribution of redox zones during lake bank filtration in Berlin, Germany. *Environ. Geol.* **2008,** *54*, (1), 53-65.